Journal of Thrombosis and Haemostasis, **16**: 1646–1655 DOI: 10.1111/jth.14193

ORIGINAL ARTICLE

Hollow organosilica beads as reference particles for optical detection of extracellular vesicles

Z. VARGA,*† E. VAN DER POL,‡§¶ M. PÁLMAI,* R. GARCIA-DIEZ,**[1] C. GOLLWITZER,**[2] M. KRUMREY,** J.-L. FRAIKIN,†† A. GASECKA,‡¶‡‡ N. HAJJI,‡ T. G. VAN LEEUWEN§¶ and R. NIEUWLAND‡¶

**Biological Nanochemistry Research Group, Institute of Materials and Environmental Chemistry, Research Center for Natural Sciences, Hungarian Academy of Sciences; †Department of Biophysics and Radiation Biology, Semmelweis University, Budapest, Hungary; ‡Laboratory of Experimental Clinical Chemistry, Academic Medical Center of the University of Amsterdam; §Department of Biomedical Engineering and Physics, Academic Medical Center of the University of Amsterdam; ¶Vesicle Observation Center, Academic Medical Center of the University of Amsterdam, Amsterdam, the Netherlands; **Physikalisch-Technische Bundesanstalt (PTB), Berlin, Germany; ††Spectradyne LLC, Torrance, CA, USA; and ‡‡1st Chair and Department of Cardiology, Medical University of Warsaw, Warsaw, Poland*

To cite this article: Varga Z, van der Pol E, Pálmai M, Garcia-Diez R, Gollwitzer C, Krumrey M, Fraikin J-L, Gasecka A, Hajji N, van Leeuwen TG, Nieuwland R. Hollow organosilica beads as reference particles for optical detection of extracellular vesicles. *J Thromb Haemost* 2018; **16**: 1646–55.

Essentials

- Standardization of extracellular vesicle (EV) measurements by flow cytometry needs improvement.
- Hollow organosilica beads were prepared, characterized, and tested as reference particles.
- Light scattering properties of hollow beads resemble that of platelet-derived EVs.
- Hollow beads are ideal reference particles to standardize scatter flow cytometry research on EVs.

Summary. *Background:* The concentration of extracellular vesicles (EVs) in body fluids is a promising biomarker for disease, and flow cytometry remains the clinically most applicable method to identify the cellular origin of single EVs in suspension. To compare concentration measurements of EVs between flow cytometers, solid polystyrene reference beads and EVs were distributed in the first ISTH-organized interlaboratory comparison studies. The beads were used to set size gates based on light scatter, and the concentration of EVs was measured within the size gates. However, polystyrene beads lead to false size determination of EVs, owing to the mismatch in refractive index between beads and EVs. Moreover, polystyrene beads gate different EV sizes on different flow cytometers. *Objective:* To prepare, characterize and test hollow organosilica beads (HOBs) as reference beads to set EV size gates in flow cytometry investigations. *Methods:* HOBs were prepared with a hard template sol-gel method, and extensively characterized for morphology, size, and colloidal stability. The applicability of HOBs as reference particles was investigated by flow cytometry with HOBs and platelet-derived EVs. *Results:* HOBs proved to be monodisperse with a homogeneous shell thickness. Two-angle light-scattering measurements by flow cytometry confirmed that HOBs have light-scattering properties similar to those of platelet-derived EVs. *Conclusions:* Because the structure and light-scattering properties HOBs resemble those of EVs, HOBs with a given size will gate EVs of the same size. Therefore, HOBs are ideal reference beads with which to standardize optical measurements of the EV concentration within a predefined size range.

Keywords: cell-derived microparticles; exosomes; extracellular vesicles; flow cytometry; microspheres.

Correspondence: Zoltán Varga, Biological Nanochemistry Research Group, Institute of Materials and Environmental Chemistry, Research Center for Natural Sciences, Hungarian Academy of Sciences, Magyar tudósok körútja 2, H-1117, Budapest, Hungary
Tel.: +36 1382 6568
E-mail: varga.zoltan@ttk.mta.hu

Present addresses: [1]*Helmholtz-Zentrum Berlin für Materialien und Energie GmbH (HZB);* [2]*Bundesanstalt für Materialforschung und -prüfung (BAM), Berlin, Germany.*

Received: 7 December 2017
Manuscript handled by: P. H. Reitsma
Final decision: P. H. Reitsma, 25 May 2018

Introduction

Extracellular vesicles (EVs), including exosomes, microvesicles, and other membrane-surrounded structures released from cells, are in the forefront of biomedical

research. Because EVs contribute to many physiological processes, EVs may serve as biomarkers for diseases, including cancer, neurological diseases, and thrombosis [1–4]. Despite the potential of EVs for diagnostic applications, gold standard techniques and reference materials for EV detection are lacking [5]. Detection of EVs is difficult, because EVs are heterogeneous in size and composition, and most EVs are smaller than 500 nm [6–8]. Throughout this article, size is defined as the diameter of the particle. Furthermore, the most widely studied body fluid with regard to EVs is blood, which contains not only EVs but similar-sized lipoprotein particles [9].

Because clinically relevant EVs are outnumbered by other EVs and lipoprotein particles, EVs are preferably characterized one by one. A recent international survey showed that optical methods are widely used to characterize single EVs [10]. Of all respondents who specified their single EV detection method, 80% used nanoparticle tracking analysis (NTA), 18% used tunable resistive pulse sensing (TRPS), and 29% used flow cytometry (bead capture assays excluded). Because only flow cytometry can identify single EVs at high throughput (> 5000 events s^{-1}) in a reproducible manner, flow cytometers hold the most promise for clinical applications.

A flow cytometer detects light scattering and fluorescence of single particles in a hydrodynamically focused fluid stream. Because flow cytometers are designed to detect cells, which are much larger than EVs, commercially available flow cytometers do not detect all EVs. The detected concentration of EVs therefore strongly depends on the sensitivity of the flow cytometer, especially because the concentration of EVs increases with decreasing size [5]. To standardize flow cytometry measurements and enable data comparison, laboratories should detect the concentration of EVs within a well-defined size range. However, the arbitrary units of flow cytometry data preclude access to the EV size, thereby impeding standardization and comparison of measurement results.

The light-scattering signals of two sizes of polystyrene beads are commonly used to gate EVs [11,12]. However, light scattering depends on the size, refractive index (RI), shape and structure of the particle, the RI of the medium, and the optical configuration of the flow cytometer. At a wavelength of 405 nm, which is used in modern flow cytometers to illuminate particles, polystyrene has an RI of 1.63, whereas EVs have an effective RI below 1.40 [13,14]. Because of this RI mismatch, 200-nm EVs scatters 40-fold to 300-fold less light than 200-nm polystyrene beads, as shown in Fig. 1. Also, 200-nm silica beads, which have an RI between 1.44 and 1.47, scatter five-fold to 50-fold more light than similar-sized EVs [14–16]. Thus, the use of solid synthetic reference beads to standardize optical measurements of EVs leads to false size assignment.

Correct sizing of EVs by scattering flow cytometry requires reference particles with light-scattering properties similar to those of EVs. EVs are concentric particles containing an approximately 4-nm phospholipid bilayer [6,17] with an RI of 1.46 ± 0.06 to 1.48 [18,19], surrounding an aqueous core with an RI close to that of water (RI of 1.34 at a wavelength of 405 nm). The ideal reference particles are therefore stable, monodisperse, concentric particles with a high-RI shell and a low-RI core.

In this study, we prepared, characterized and applied hollow organosilica beads (HOBs) with nominal sizes of 200 nm (HOB200) and 400 nm (HOB400) as reference materials for optical detection of EVs. Because of their concentric structure and organosilica shell, HOBs have an RI distribution resembling that of EVs. On the basis of Mie theory, HOBs are expected to have similar light-scattering properties to those of EVs, as shown in Fig. 1. The goals of this study were to: (i) determine the size distribution, concentration, structure, colloidal stability and light-scattering properties of the prepared HOBs; (ii) confirm that HOBs have light-scattering properties similar to those of EVs from blood plasma; and (iii) use the HOBs to set a size gate that is independent of the collection angles of a flow cytometer.

Methods

Preparation of HOBs

1,2-Bis(triethoxysilyl)ethane (BTEE) (96%; Sigma-Aldrich, St Louis, MO, USA), cyclohexane (Guaranteed Reagent, 99.99%; Lach-Ner, Neratovice, Czech Republic), and L-arginine (reagent grade, ≥ 98%, TLC; Sigma-Aldrich) were used. Silica dispersions of 200 nm (PSI-0.2) and 400 nm (PSI-0.4) in water were obtained from Kisker Biotech (Steinfurt, Germany). High-purity deionized water (18.2 MΩ cm^{-1}) was used during synthesis.

HOBs were synthesized by combining a basic amino acid catalysis route with a hard template approach in a 4-mL glass vial [20,21]. Briefly, 2.6 mg of L-arginine and 300 μL of silica dispersion (50 mg mL^{-1}) serving as the template particles were added to 1.7 mL of water. Then, 130 μL of cyclohexane was overlayered on the aqueous phase, and 134 μL of BTEE, the precursor of the organosilica shell, was injected into the non-polar phase. The reaction mixture was allowed to react under vigorous stirring (500 r.p.m.) at 60 °C for 24 h. Then, cyclohexane was removed, the pH was adjusted to 12.75 ± 0.05 by addition of 150 μL of 1 mol L^{-1} NaOH solution, and the dispersion was stirred for 24 h at room temperature in order to etch the template silica core. The mesoporous shell structure and hydrolytic stability of organosilica under basic conditions enables etching of the silica core while maintaining the shell integrity. Finally, the sample was transferred into a 2-mL Slide-A-Lyzer MINI Dialysis Device (20K MWCO;

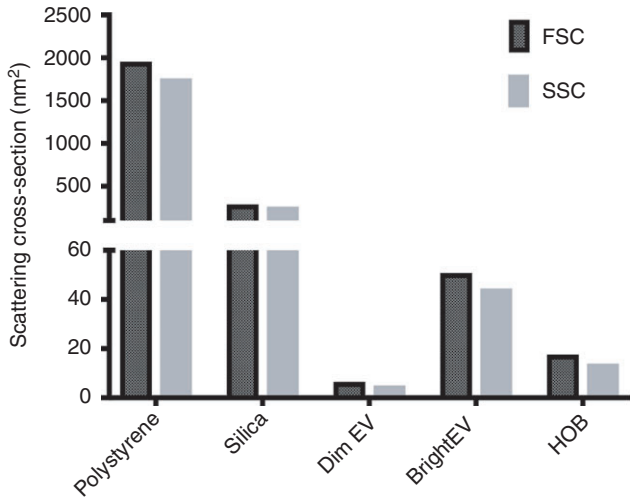

Fig. 1. Theoretical forward scatter (FSC) and side scatter (SSC) cross-sections of polystyrene beads, silica beads, dim and bright extracellular vesicles (EVs) and hollow organosilica beads (HOBs) for an Apogee A60-Micro flow cytometer. The model calculations were performed according to Mie scattering theory. The following refractive indices at a wavelength of 405 nm were used for the calculations: 1.63 for polystyrene, 1.46 for silica, 1.48 for the EV shell, 1.34 for the core of dim EVs, 1.38 for the core of bright EVs, 1.46 for the HOB shell, and 1.34 for the HOB core. The particle size (diameter) was 200 nm in all cases, and the shell thickness was set to 5 nm for EVs and 10 nm for HOBs.

Thermo Fisher Scientific, Waltham, MA, USA) and dialysed against 42.5 mL of water for four times in 2 days to remove NaOH and side products.

Preparation and storage of cell-depleted plasma

Citrate-anticoagulated blood (0.32%) was collected from 10 healthy individuals (five males and five females; age 45 ± 12 years [mean ± standard deviation]) with informed consent by venipuncture without a tourniquet through a 21-gauge needle by use of a vacutainer system. To remove cells, blood was centrifuged twice (1550 × *g*, 20 min, 20 °C) with a Rotina 380 R centrifuge equipped with a swing-out rotor and a radius of 155 mm (Hettich Zentrifugen, Tuttlingen, Germany). The centrifugation parameters were 1550 × *g* for 20 min at 20 °C, an acceleration speed of 1, and no brake. After a single centrifugation, plasma was transferred to a new 5-mL plastic tube, leaving ~ 1 cm of plasma above the buffy layer. After the second centrifugation, plasma was collected and transferred carefully to a new 5-mL plastic tube, leaving ~ 100 μL at the bottom of the old tube. The number of remaining platelets after the second centrifugation is, on average, 0.5% of the initial platelet count in whole blood (n = 4; data not shown), which is similar to the recommended ISTH protocol (2 × 2500 × *g* for 15 min at 20 °C) [11]. Although our protocol and the ISTH protocol give similar results with regard to remaining platelets, we recommend using the ISTH protocol to circumvent confusion and to enable the comparison of results between studies and laboratories [22]. Aliquots of 100 μL of cell-depleted plasma were snap-frozen in liquid nitrogen for 15 min, and stored at − 80 °C until use. After thawing on ice, 20 μL of plasma was incubated in the dark for 120 min at 20 °C with 2.5 μL of phycoerythrin (PE)-conjugated CD61 or IgG_1–PE control (555754 and 340013, respectively; both 6.25 μg mL^{-1}; Becton Dickinson, San Jose CA, USA). Labeling was stopped by addition of 200 μL of 50-nm-filtered (Whatman, Maidstone, UK), citrate-containing (0.32%) phosphate-buffered saline (PBS) (pH 7.4). To verify the presence of EVs, cell-depleted plasma was characterized by NTA and transmission electron microscopy (TEM) (Fig. S1).

TEM

Morphological investigations of HOBs were carried out on a MORGAGNI 268D (FEI, Eindhoven, the Netherlands) transmission electron microscope. Diluted sample was dropped and dried on a carbon-coated copper grid. Figure S1 legend contains the TEM protocol for EVs from cell-depleted plasma.

Dynamic light scattering (DLS)

HOBs were characterized by DLS (W130i Dynamic Light Scattering System; AvidNano, High Wycombe, UK). Samples were diluted 50-fold with ultrapure water (Merck Millipore, Billerica, MA, USA). Low-volume disposable plastic cuvettes were used for the DLS measurements (UVette; Eppendorf Austria, Vienna, Austria), and data evaluation was performed with ISIZE 3.0 software (AvidNano), utilizing the CONTIN algorithm.

Small-angle X-ray scattering (SAXS)

Hollow organosilica beads were characterized by SAXS at the four-crystal monochromator beamline of PTB [23,24] at the synchrotron radiation facility BESSY II (Helmholtz-Zentrum Berlin, Germany). The mean size, size distribution and shell thickness of HOBs were determined by least-squares fitting of a model function to the experimentally measured scattering curves (Data S1; Fig. S2) [25,26].

Zeta potential

Zeta potential measurements of HOBs were performed by use of a Zetasizer Nano ZS (Malvern Instruments, Malvern, UK) equipped with an He–Ne laser (λ = 633 nm) and a backscatter detector at a fixed angle of 173°.

NTA

A dark-field microscope (NS500; Nanosight, Amesbury, UK) with a 45-mW 405-nm laser and an electron-

multiplying charge-coupled device was used to determine the size and concentration of HOBs by NTA. Samples were diluted 10 000-fold (HOB200) or 100-fold (HOB400) in 50-nm-filtered (Whatman) deionized water. For each sample, 30 videos of 10 s were captured at 22.0 °C with camera level 15 (HOB200) or 12 (HOB400) [22]. Data were analyzed with NTA 3.1 BUILD 3.1.54 (Nanosight), on the assumption of a medium viscosity of 0.95 cP and with a threshold of 10 gray values. Figure S1 legend contains the NTA protocol for EVs from cell-depleted plasma.

TRPS

TRPS (qNano; Izon Science, Oxford, UK) was used to determine the size and concentration of HOBs. Samples were diluted 500-fold (HOB200) or 50-fold (HOB400) in 50-nm-filtered (Whatman) PBS. HOBs were measured with NP200 (HOB200) and NP400 (HOB400) nanopores. The voltage was adjusted between 0.40 V and 0.70 V to obtain a baseline current of 125 nA with a nanopore stretch of 47.00 mm [27]. Then, the stretch was adjusted such that the amplitude of the resistive pulses of reference beads (Izon Science) was within the range recommended by the manufacturer. This resulted in a stretch between 45.50 mm and 47.00 mm. Finally, the voltage was adjusted between 0.40 V and 0.70 V to get the baseline current as close as possible to 125 nA. Samples were measured with an external pressure of 7.0 mbar, and at least 1000 beads per sample were analyzed. Particle size and concentration were calibrated with reference beads (Izon Science). Data acquisition and processing were performed with IZON CONTROL SUITE version 3.2.2.268.

Microfluidic resistive pulse sensing (MRPS)

MRPS (nCS1; Spectradyne LLC, Torrance, CA, USA) was used to determine the size and concentration of HOBs [28]. Samples were diluted 1000-fold (HOB200) or 100-fold (HOB400) in 50-nm-filtered (Whatman) PBS containing 0.6 mmol L^{-1} SDS. All samples were measured with a TS-900 cartridge at a voltage of 4 V. To relate the frequency of resistive pulses to the particle concentration, 695-nm reference beads (Spectradyne) with a concentration of 2×10^8 mL^{-1} were used.

Flow cytometry

A flow cytometer (A60-Micro; Apogee, Hemel Hempstead, UK) equipped with a 200-mW 405-nm laser was used to detect forward-scattered light, side-scattered light and fluorescence of beads and EVs. Side scatter (SSC) was used as the trigger channel, with the threshold at 14 arbitrary units. For the forward scatter (FSC), SSC and PE fluorescence channels, the gain was 1 and the voltages were 380 V, 375 V, and 520 V, respectively. Samples were measured for 1 min at a flow rate of 3.01 μL min^{-1} and with a sheath pressure of 150 mbar. Rosetta Calibration (Exometry, Amsterdam, the Netherlands) was used to relate SSC to the size and RI of nanoparticles according to Mie theory [29]. To validate this relationship, the SSC of silica beads (Kisker Biotech) was measured at a concentration of 10^7 mL^{-1}. Median fluorescence intensity was related to molecules of equivalent soluble fluorochrome (MESF) for PE by use of the SPHERO PE Calibration kit (ECFP-F2-5K; Spherotech, Lake Forest, IL, USA). Figure S3 shows the relationship between the measured PE intensity in arbitrary units and MESF, which was obtained by least square fitting the logarithm of the data. The gate of the PE channel was set at 51 MESF. HOB200 and HOB400 were diluted 10^5-fold and 10^3-fold in purified water to detected concentrations of 6.7×10^6 mL^{-1} and 1.4×10^7 mL^{-1}, respectively. Cell-depleted plasma was diluted 66-fold in PBS to avoid swarm detection, as confirmed by serial dilutions [30]. For the cell-depleted plasma, data of five measurements were combined to create the scatter plot shown in Fig. 5. Data acquisition was performed with Apogee software, and data were processed with FLOWJO v.10.3 (FlowJo LLC, Ashland, OR, USA).

Results

Size distribution of HOBs

The prepared HOBs were characterized by TEM, NTA, TRPS, MRPS, DLS, and SAXS. TEM images showed that HOBs had homogeneous morphology and uniform layer thicknesses (Fig. 2). Figure 3 shows the size distributions of HOBs obtained with the single particle detection methods TEM, NTA, TRPS, and MRPS. Among ensemble techniques, DLS resulted in mean sizes of 188 nm and 356 nm, and full-width-at-half-maximum (FWHM) values of 52 nm and 118 nm for HOB200 and HOB400, respectively. SAXS, which is the only traceable method used in this study, resulted in mean sizes (value ± uncertainty) of 189 ± 2 nm and 374 ± 10 nm for HOB200 and HOB400, respectively. SAXS gave a polydispersity (FWHM/mean) below 15%. Table S1 shows a summary of all size measurements.

Concentration, structure and stability of HOBs

NTA, TRPS, MRPS and flow cytometry gave concentrations of 2.2×10^{12}, 2.0×10^{11}, 2.7×10^{11}, and 6.7×10^{11} particles per milliliter for HOB200, and 4.4×10^{10}, 1.6×10^{10}, 1.4×10^{10} and 1.4×10^{10} particles per milliliter for HOB400, respectively.

Besides size, SAXS provides information on the structure and electron density distribution of HOBs. By fitting a core–shell model to the measured scattering curves, we obtained shell thicknesses of 8.1 ± 0.5 nm for HOB200

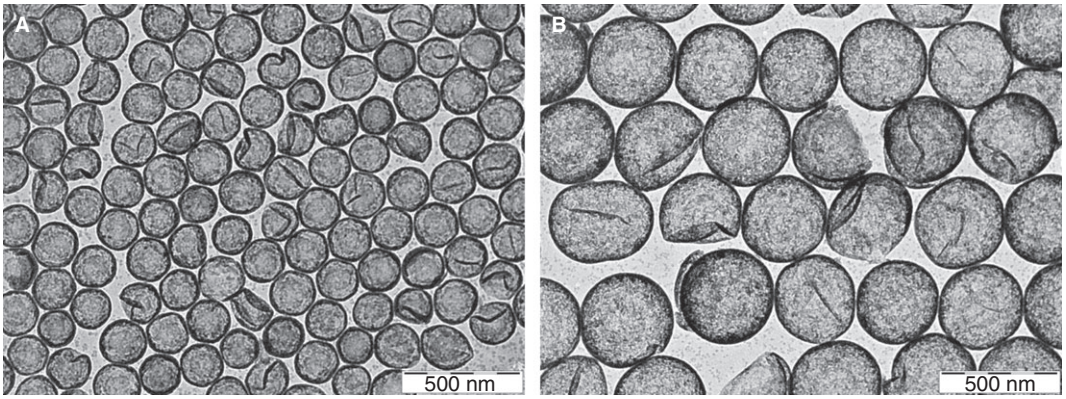

Fig. 2. Transmission electron microscopy (TEM) analysis of hollow organosilica beads (HOBs). TEM images of HOBs prepared by the use of nominal 200-nm (A) and 400-nm (B) silica templates.

and 6.4 ± 0.7 nm for HOB400. Furthermore, we obtained an average electron density of the core of 345 nm^{-3} for both samples, which is close to the electron density of water (333 nm^{-3}). This observation confirms the successful etching of the template silica core.

The colloidal stability of the HOBs, which describes the aggregation properties of the beads, was evaluated by zeta potential measurements. We found highly negative zeta potentials (− 56.6 mV for HOB200 and − 58.1 mV for HOB400), which we associated with the dissociation of surface silanol groups [31]. The highly negative zeta potentials suggest that HOBs have excellent colloidal stability in water at pH 7.4.

Light-scattering properties of HOBs measured by flow cytometry

To test the applicability of HOBs as reference particles for characterization of EVs by flow cytometry, we compared the light-scattering properties of HOBs and EVs. Figure 4A shows the side-scattering intensity of polystyrene beads, silica beads and HOBs measured by flow cytometry and calculated according to Mie theory. Whereas the polystyrene beads (coefficient of determination, $R^2 = 1.00$) and silica beads ($R^2 = 0.97$) were well described by a solid-sphere Mie model, the HOBs ($R^2 = 0.95$) were well described by a hollow-sphere Mie model. By least square fitting the theory to the data, we obtained a shell thickness of 10.1 nm for the HOBs, which is close to the shell thickness determined by SAXS. Because of the hollow structure, HOBs scatter at least an order of magnitude less light than similar-sized solid silica beads. The scattering intensity of HOBs thereby overlaps with the scattering intensity expected from EVs. We modeled EVs as concentric particles with a 4-nm shell (RI = 1.48) [32–36] and a core ($1.35 \leq RI \leq 1.37$) [37–40]. The RI range of the core corresponds to a realistic protein concentration between 10% and 20% [41]. Our model parameters resulted in scattering intensities similar to those of platelet-derived EVs, with a median RI of 1.37 and a mode RI of 1.39 at 405 nm, which was previously measured under the assumption that EVs have a homogeneous RI distribution [13,42]. More accurate estimates of the RI distribution of EVs require monodisperse EV populations, which are currently unavailable.

To demonstrate that HOBs have light-scattering properties similar to those of EVs, Fig. 4B shows the measured SSC intensity versus FSC intensity for HOBs, platelet-derived ($CD61^+$) EVs from cell-depleted plasma, and, for comparison, 125-nm polystyrene beads and 182-nm and 402-nm silica beads. As a reference, the arrows relate the size range of EVs expected from Mie theory to their FSC and SSC values. The data show that, for a given FSC of this flow cytometer, HOBs have low SSC whereas polystyrene and silica beads have high SSC as compared with EVs. However, HOBs are within the theoretical EV size range, and are therefore expected to be better reference materials with which to standardize flow cytometry measurements on EVs.

HOBs outperform solid beads for standardization of EV flow cytometry

To demonstrate that HOBs can be used to determine the EV concentration independently of the light-scattering

Fig. 3. Size (diameter) distributions of nominal 200-nm and 400 nm sized hollow organosilica beads (HOBs) obtained with single particle detection methods. (A, B) Transmission electron microscopy (TEM); 10-nm bin width. (C, D) Nanoparticle tracking analysis (NTA); 1-nm bin width; the gray area represents the standard deviation. (E, F) Tunable resistive pulse sensing (TRPS); 10-nm bin width. (G, H) Microfluidic resistive pulse sensing (MRPS); the error bars represent the standard deviation; 10-nm bin width. Mean sizes and full-width-at-half-maximum (FWHM) values from Gaussian fits of the distributions are indicated for each method. In the case of HOB400, a shoulder can be seen on the distributions, which might be attributable to incomplete particles or polycondensation of the organosilica precursor during synthesis. [Color figure can be viewed at wileyonlinelibrary.com]

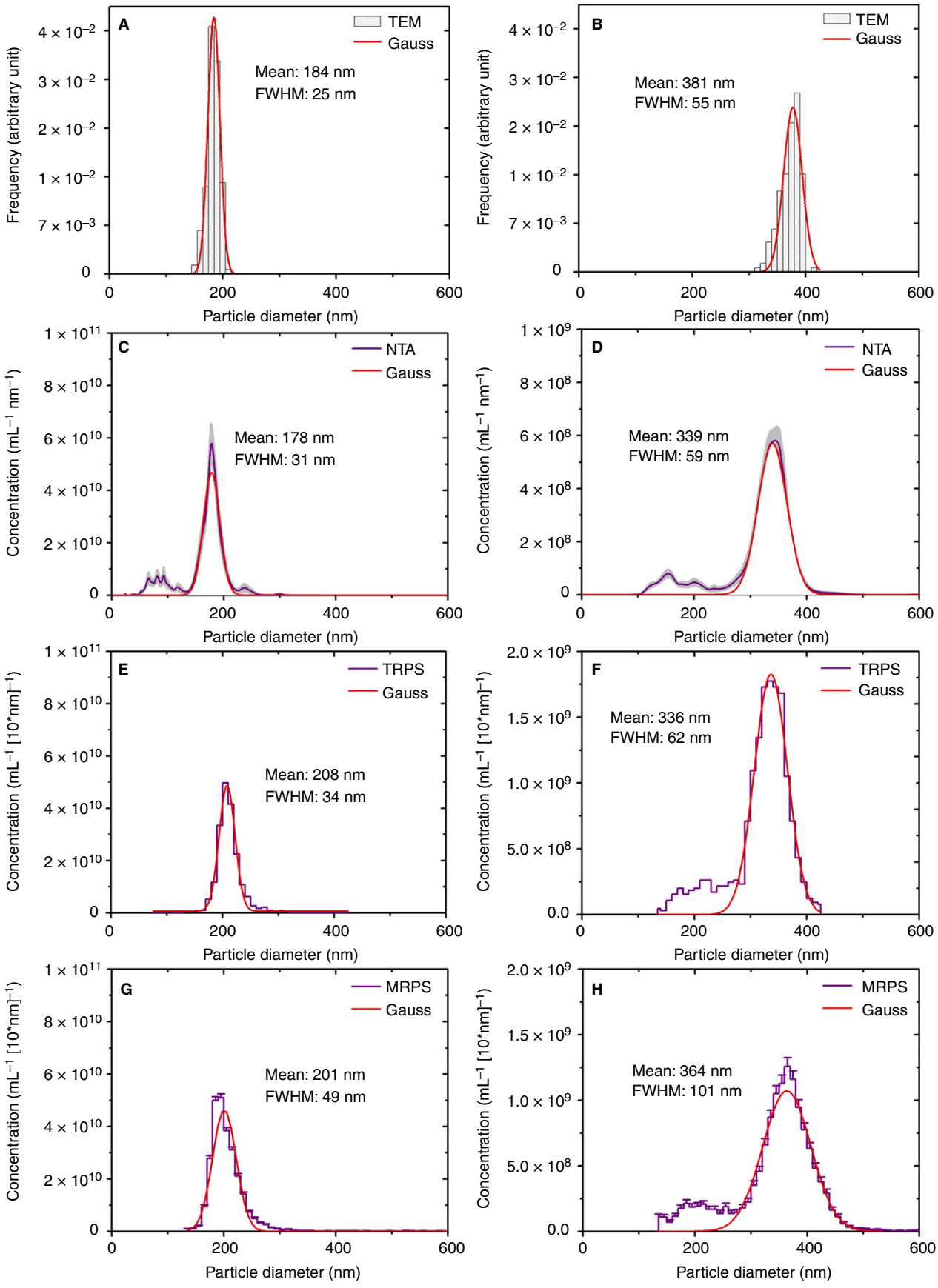

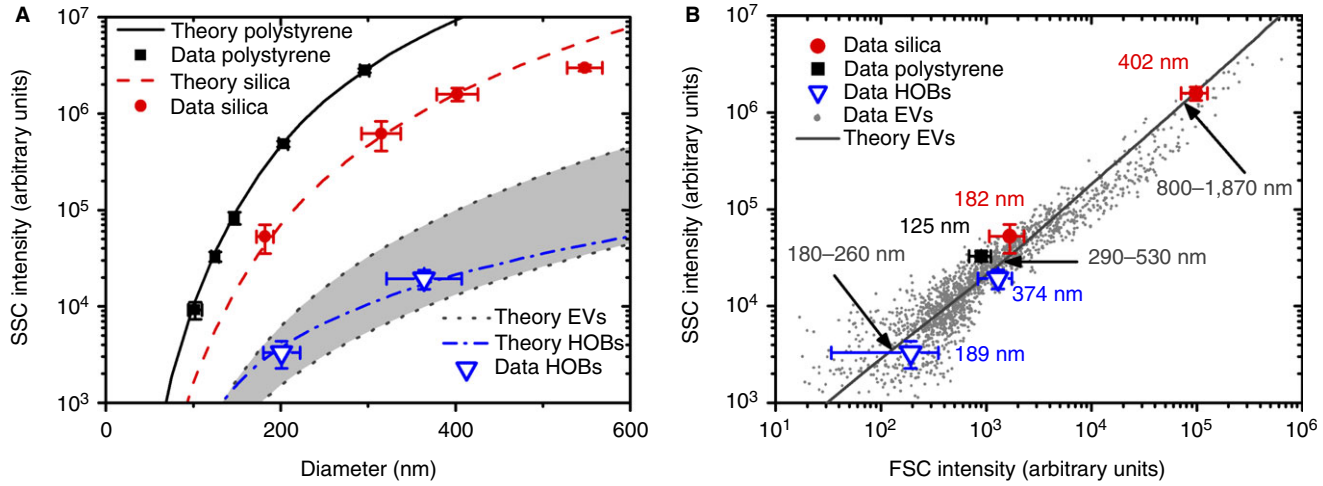

Fig. 4. Light-scattering properties of polystyrene beads (squares), silica beads (circles), hollow organosilica beads (HOBs; triangles) and platelet-derived ($CD61^+$) extracellular vesicles (EVs; dots) from human plasma measured (symbols) by flow cytometry and calculated (lines) according to Mie theory. (A) Side scatter (SSC) versus size (diameter). Whereas polystyrene and silica beads scatter orders of magnitudes more light than similar-sized EVs, the properties of HOBs resemble the expected SSC properties of EVs (gray area). (B) SSC versus forward scatter (FSC). In contrast to polystyrene and silica beads, HOBs have FSC and SSC intensities similar to those of EVs of the same size. Data points and error bars represent the mean and standard deviation, respectively. The arrows relate the size range of EVs expected from Mie theory to their FSC and SSC values. Size ranges are based on the SSC confidence interval (gray area) for EVs in (A). The following refractive indices at a wavelength of 405 nm were used for the calculations: 1.63 for polystyrene, 1.46 for silica, 1.48 for the EV shell, 1.35 and 1.37 for the EV core, to obtain the lower and upper boundaries of the gray area in (A), respectively, 1.36 for the EV core in (B), 1.48 for the HOB shell, and 1.34 for the water. Least square fitting resulted in a shell thickness of 10.1 nm for the HOBs. [Color figure can be viewed at wileyonlinelibrary.com]

collection angles of a flow cytometer, we determined the concentration of platelet-derived EVs by using the FSC or SSC detector within size gates set by HOBs. Because the sensitivity and the scatter-to-size relationship differ between the FSC and SSC detectors of our flow cytometer [5], whereas the flow rate and sample composition are the same for both detectors, we hoped that this experiment would demonstrate that HOBs set an EV size gate independently of the collection angles. Figure 5 shows the concentrations of platelet-derived EVs within gates set by polystyrene beads, silica beads and HOBs for the FSC and SSC detectors. Figure S4 shows the applied gates for Figure 4B. The percentage difference in the gated concentration from the mean concentration was smallest for the gates set by HOBs as compared with solid beads, suggesting that HOBs outperform solid beads for the standardization of EV flow cytometry.

Discussion

Standardization of flow cytometry measurements is essential to explore the diagnostic potential of EVs. As the scattering intensities measured by flow cytometry are in arbitrary units, there is a need for reference beads with a known size and light-scattering properties similar to those of EVs. The optical properties of a particle depend not only on the size but also on the RI distribution within the particle. EVs typically have a 4-nm-thick shell with a high RI and a core with a low RI. In contrast, polystyrene and silica beads consist of a homogeneously distributed high-RI material, and therefore scatter orders of magnitude more light than similar-sized EVs (Fig. 4A). In this article, we introduce HOBs with light-scattering properties similar to those of EVs to standardize optical measurements on EVs.

HOBS with smooth surfaces were produced by optimizing the existing hard template approach proposed by Koike *et al.* [20]. All established particle measurement methods (TEM, NTA, TRPS, and SAXS) confirmed a narrow size distribution (FWHM/mean < 0.25) of HOBs. The relative standard deviation of the mean size values obtained with the different methods is < 10%, which indicates good agreement between the methods used. All methods indicate the presence of contaminants, which are smaller than HOBs and have a lower concentration. These contaminants might originate from incomplete particles or from the polycondensation of the organosilica precursor. Introducing a further purification step during the synthesis may eliminate these contaminants.

The hollow core–shell structure of the prepared HOBs was confirmed by TEM and SAXS, and indirectly by flow cytometry. NTA, TRPS, MRPS and flow cytometry were also used to determine the concentrations of the prepared HOBs. The obtained values show an order of magnitude deviation for HOB200 and a factor of 3.4 deviation for HOB400. However, concentration measurements require careful interpretation, especially because no standards or primary methods exist and no certified reference materials are available for the concentration determination of nanoparticles [43].

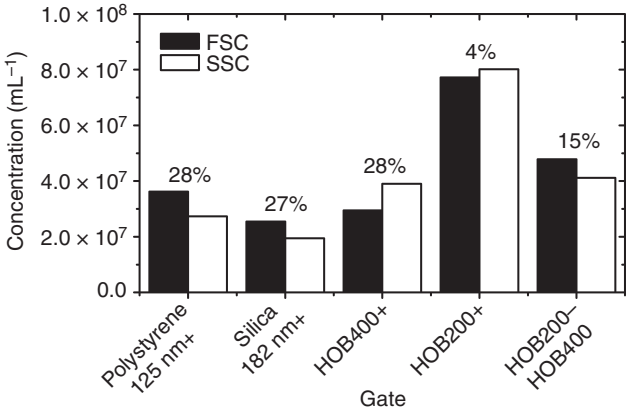

Fig. 5. Concentrations of platelet-derived extracellular vesicles within gates set by polystyrene beads, silica beads, and hollow organosilica beads (HOBs) for the forward scatter (FSC) and side scatter (SSC) detectors. Concentrations are corrected for sample dilutions. For the first four gates, the indicated bead is used as the lower size gate, and no upper size gate is applied. For the HOB200–HOB400 gate, HOB200 and HOB400 are used as the lower and upper size gates, respectively. The numbers above the bars indicate the percentage difference in the gated concentration relative to the mean concentration.

Flow cytometry measurements show that HOBs scatter approximately an order of magnitude less light than similar-sized solid silica beads (Fig. 4A). The measured light scatter of HOBs thereby overlaps with the expected light scatter for EVs, which is also expected, given the spatial RI distribution within both particle types. To demonstrate that HOBs and EVs do indeed have similar light-scattering properties, we measured the FSC and SSC of HOBs and platelet-derived EVs from blood plasma (Fig. 4B). We found that HOBs have low SSC (or high FSC), whereas polystyrene and silica beads have high SSC (or low FSC), as compared with EVs. However, the shell thickness of HOBs can, in principle, be tuned to exactly match the FSC and SSC properties of EVs. Moreover, HOBs are closer to the theoretical EV size, which emphasizes the wrong size assignment of EVs when solid reference beads are used to set gates. For example, 182-nm solid silica beads produce SSC and FSC signals that are comparable to those produced by 374-nm HOBs, meaning that a two-fold difference in size assignment between solid and hollow silica beads exists.

To confirm the above findings, we applied HOBs to set size gates on FSC and SSC, which collect light over different collection angles, resulting in totally different scatter–size relationships [5]. Figure 5 shows that the variation in the gated EV concentrations of these detectors was minimal for gates set by HOBs, confirming that HOBs have similar optical properties to EVs and, in fact, define an EV gate in nanometers. A multicenter and multiflow cytometer follow-up study is required to demonstrate the superiority of HOBs over solid beads.

The illumination wavelength of our flow cytometer is 405 nm. We expect that EV size gates set by HOBs will also be applicable to flow cytometers with other common illumination wavelengths, such as 375 nm and 488 nm. The RIs of glass and water at 375 nm are almost 0.01 higher than the RIs of glass and water at 488 nm. However, scattering depends on the RI contrast, in this case between water and the shell of the HOBs or EVs. Because, within this wavelength range, the dispersion relationships of glass and water have similar slopes, the RI contrasts between water and glass remain similar, at 375 nm and 488 nm [44,45]. The dispersion relationship of the shell of EVs is unknown, but, on the basis of the dispersion relationships of organic materials, negligible changes in the RI contrast between water and the shell of EVs is expected between 375 nm and 488 nm.

An alternative to setting EV size gates with HOBs is to relate the scattering intensity of solid polystyrene and silica reference beads to that of EVs by the use of Mie theory [29]. Mie theory accounts for RI differences, but requires complex software and knowledge of the optical configuration of the flow cytometer. HOBs are more practical to use, because HOBs can directly be used to set an EV size gate in nanometers, owing to the almost similar light-scattering properties of EVs and HOBs. Perhaps the best solution would be the use of Mie theory in combination with HOBs to allow the user flexibility in selection of an EV size gate by flow cytometry.

Conclusions

In summary, we introduced HOBs to be used as reference beads for optical characterization of EVs. Thorough characterization of the prepared HOBs revealed narrow size distributions, colloidal stability, and a homogeneous hollow core–shell structure of HOBs. The safety, monodispersity and stability of HOBs are superior to those of potential biological reference particles [46], which, like HOBs, have light-scattering properties resembling those of EVs. The flow cytometry investigations confirmed that HOBs have similar light-scattering properties to those of EVs, and are therefore more suitable as reference beads for flow cytometry characterization of EVs than solid polystyrene or silica beads. HOBs can be used to set size gates in nanometers independently of the optical configuration of a flow cytometer. Therefore, HOBs are ideal reference beads with which to standardize optical measurements of the EV concentration within a predefined size range, which may facilitate the comparison of EV measurements between instruments and institutes.

Addendum

Z. Varga and E. van der Pol designed and performed the research, and wrote the paper. M. Pálmai contributed to the synthesis and characterization. R. Garcia-Diez, C.

Gollwitzer, and M. Krumrey performed the SAXS analysis and contributed to writing the paper. J.-L. Fraikin performed MRPS analysis. A. Gasecka and N. Hajji contributed to characterization. T. G. van Leeuwen contributed to writing the paper. R. Nieuwland designed the research and contributed to writing the paper.

Acknowledgements

We thank C. Hau and L. Rikkert (Laboratory of Experimental Clinical Chemistry, Academic Medical Center, University of Amsterdam, Amsterdam, the Netherlands) for the TEM investigation of the cell-depleted plasma sample. This work was supported by the National Research, Development and Innovation Office (Hungary) under grant numbers PD 121326 and NVKP_16-1-2016-0007. Z. Varga was supported by the János Bolyai Research Fellowship of the Hungarian Academy of Sciences. Part of this work was supported by the Cancer-ID program (www.utwente.nl/tnw/cancer-id), the MEMPHISII program of the Netherlands Technology Foundation STW, and the VENI program (15924, E. van der Pol) of the Netherlands Organization for Scientific Research – Domain Applied and Engineering Sciences (NWO-TTW).

Disclosure of Conflict of Interests

E. van der Pol is co-founder and shareholder of Exometry B.V. J.-L. Fraikin is co-founder of Spectradyne LLC, which developed the nCS1 instrument used in the study. The other authors state that they have no conflict of interest.

Supporting Information

Additional supporting information may be found online in the Supporting Information section at the end of the article:

Fig. S1. Size distribution of all particles in the cell-depleted plasma by (A) nanoparticle tracking analysis, and (B) transmission electron microscopy.
Fig. S2. Experimental scattering curves (black circles) of the (A) HOB200 and (B) HOB400 samples and their corresponding fit displayed as a red line.
Fig. S3. Molecules of equivalent soluble fluorochrome (MESF) versus median fluorescence intensity of the phycoerythin (PE) channel.
Fig. S4. Side scatter versus phycoerythrin (PE) fluorescence (A,C,E,G,I,K) and side scatter versus forward scatter (B,D,F,H,J,L) for plasma extracellular vesicles labeled with CD61 and the isotype control measured by flow cytometry. The vertical line at 51 MESF indicates the gate of the PE channel.
Table S1. Mean diameters and the full-width-at-half-maximum values (FWHMs) of the size distributions of HOBs obtained by transmission electron microscopy (TEM), dynamic light scattering (DLS), particle tracking analysis (PTA), tunable and microfluidic resistive pulse sensing (RPS), and small-angle X-ray scattering (SAXS). In the case of SAXS, the estimated uncertainty is given for the mean diameter value.
Data S1. SAXS model.

References

1 van Eijndhoven MAJ, Zijlstra JM, Groenewegen NJ, Drees EEE, van Niele S, Baglio SR, Koppers-Lalic D, van der Voorn H, Libregts SFWM, Wauben MHM, de Menezes RX, van Weering JRT, Nieuwland R, Visser L, van den Berg A, de Jong D, Pegtel DM. Plasma vesicle miRNAs for therapy response monitoring in Hodgkin lymphoma patients. *JCI Insight* 2016; **1**: e89631.
2 Hoshino A, Costa-Silva B, Shen T-L, Rodrigues G, Hashimoto A, Tesic Mark M, Molina H, Kohsaka S, Di Giannatale A, Ceder S, Singh S, Williams C, Soplop N, Uryu K, Pharmer L, King T, Bojmar L, Davies AE, Ararso Y, Zhang T, *et al*. Tumour exosome integrins determine organotropic metastasis. *Nature* 2015; **527**: 329–35.
3 Melo SA, Luecke LB, Kahlert C, Fernandez AF, Gammon ST, Kaye J, LeBleu VS, Mittendorf EA, Weitz J, Rahbari N, Reissfelder C, Pilarsky C, Fraga MF, Piwnica-Worms D, Kalluri R. Glypican-1 identifies cancer exosomes and detects early pancreatic cancer. *Nature* 2015; **523**: 177–82.
4 van der Pol E, Böing AN, Gool EL, Nieuwland R. Recent developments in the nomenclature, presence, isolation, detection and clinical impact of extracellular vesicles. *J Thromb Haemost* 2016; **14**: 48–56.
5 van der Pol E, Coumans FAW, Grootemaat AE, Gardiner C, Sargent IL, Harrison P, Sturk A, van Leeuwen TG, Nieuwland R. Particle size distribution of exosomes and microvesicles determined by transmission electron microscopy, flow cytometry, nanoparticle tracking analysis, and resistive pulse sensing. *J Thromb Haemost* 2014; **12**: 1182–92.
6 Arraud N, Linares R, Tan S, Gounou C, Pasquet J-M, Mornet S, Brisson AR. Extracellular vesicles from blood plasma: determination of their morphology, size, phenotype and concentration. *J Thromb Haemost* 2014; **12**: 614–27.
7 Brisson AR, Tan S, Linares R, Gounou C, Arraud N. Extracellular vesicles from activated platelets: a semiquantitative cryo-electron microscopy and immuno-gold labeling study. *Platelets* 2017; **28**: 263–71.
8 Varga Z, Yuana Y, Grootemaat AE, van der Pol E, Gollwitzer C, Krumrey M, Nieuwland R. Towards traceable size determination of extracellular vesicles. *J Extracell Vesicles* 2014; **3**: 23298.
9 Sódar BW, Kittel Á, Pálóczi K, Vukman KV, Osteikoetxea X, Szabó-Taylor K, Németh A, Sperlágh B, Baranyai T, Giricz Z, Wiener Z, Turiák L, Drahos L, Pállinger É, Vékey K, Ferdinandy P, Falus A, Buzás EI. Low-density lipoprotein mimics blood plasma-derived exosomes and microvesicles during isolation and detection. *Sci Rep* 2016; **6**: 24316.
10 Gardiner C, Di Vizio D, Sahoo S, Théry C, Witwer KW, Wauben M, Hill AF. Techniques used for the isolation and characterization of extracellular vesicles: results of a worldwide survey. *J Extracell Vesicles* 2016; **5**: 32945.
11 Lacroix R, Robert S, Poncelet P, Kasthuri RS, Key NS, Dignat-George F, ISTH SSC Workshop. Standardization of platelet-derived microparticle enumeration by flow cytometry with calibrated beads: results of the International Society on Thrombosis and Haemostasis SSC Collaborative workshop. *J Thromb Haemost* 2010; **8**: 2571–4.

12 Cointe S, Judicone C, Robert S, Mooberry MJ, Poncelet P, Wauben M, Nieuwland R, Key NS, Dignat-George F, Lacroix R. Standardization of microparticle enumeration across different flow cytometry platforms: results of a multicenter collaborative workshop. *J Thromb Haemost* 2017; **15**: 187–93.
13 Gardiner C, Shaw M, Hole P, Smith J, Tannetta D, Redman CW, Sargent IL. Measurement of refractive index by nanoparticle tracking analysis reveals heterogeneity in extracellular vesicles. *J Extracell Vesicles* 2014; **3**: 25361.
14 van der Pol E, Coumans FA, Sturk A, Nieuwland R, van Leeuwen TG. Refractive index determination of nanoparticles in suspension using nanoparticle tracking analysis. *Nano Lett* 2014; **14**: 6195–201.
15 Parida BK, Garrastazu H, Aden JK, Cap AP, McFaul SJ. Silica microspheres are superior to polystyrene for microvesicle analysis by flow cytometry. *Thromb Res* 2015; **135**: 1000–6.
16 Chandler WL, Yeung W, Tait JF. A new microparticle size calibration standard for use in measuring smaller microparticles using a new flow cytometer. *J Thromb Haemost* 2011; **9**: 1216–24.
17 Issman L, Brenner B, Talmon Y, Aharon A. Cryogenic transmission electron microscopy nanostructural study of shed microparticles. *PLoS ONE* 2013; **8**: e83680.
18 van Manen H-J, Verkuijlen P, Wittendorp P, Subramaniam V, van den Berg TK, Roos D, Otto C. Refractive index sensing of green fluorescent proteins in living cells using fluorescence lifetime imaging microscopy. *Biophys J* 2008; **94**: L67–9.
19 Beuthan J, Minet O, Helfmann J, Herrig M, Müller G. The spatial variation of the refractive index in biological cells. *Phys Med Biol* 1996; **41**: 369–82.
20 Koike N, Ikuno T, Okubo T, Shimojima A. Synthesis of monodisperse organosilica nanoparticles with hollow interiors and porous shells using silica nanospheres as templates. *Chem Commun* 2013; **49**: 4998–5000.
21 Hartlen KD, Athanasopoulos APT, Kitaev V. Facile preparation of highly monodisperse small silica spheres (15 to >200 nm) suitable for colloidal templating and formation of ordered arrays. *Langmuir* 2008; **24**: 1714–20.
22 Coumans FAW, Brisson AR, Buzas EI, Dignat-George F, Drees EEE, El-Andaloussi S, Emanueli C, Gasecka A, Hendrix A, Hill AF, Lacroix R, Lee Y, van Leeuwen TG, Mackman N, Mäger I, Nolan JP, van der Pol E, Pegtel DM, Sahoo S, Siljander PRM, *et al*. Methodological guidelines to study extracellular vesicles. *Circ Res* 2017; **120**: 1632–48.
23 Krumrey M, Ulm G. High-accuracy detector calibration at the PTB four-crystal monochromator beamline. *Nucl Instrum Methods Phys Res Sect Accel Spectrometers Detect Assoc Equip* 2001; **467**: 1175–8.
24 Gleber G, Cibik L, Haas S, Hoell A, Müller P, Krumrey M. Traceable size determination of PMMA nanoparticles based on small angle X-ray scattering (SAXS). *J Phys Conf Ser* 2010; **247**: 012027.
25 Varga Z, Yuana Y, Grootemaat AE, van der Pol E, Gollwitzer C, Krumrey M, Nieuwland R. Towards traceable size determination of extracellular vesicles. *J Extracell Vesicles* 2014; **3**: 23298.
26 van der Pol E, Coumans F, Varga Z, Krumrey M, Nieuwland R. Innovation in detection of microparticles and exosomes. *J Thromb Haemost* 2013; **11**: 36–45.
27 Coumans FAW, van der Pol E, Böing AN, Hajji N, Sturk G, van Leeuwen TG, Nieuwland R. Reproducible extracellular vesicle size and concentration determination with tunable resistive pulse sensing. *J Extracell Vesicles* 2014; **3**: 25922.
28 Fraikin J-L, Teesalu T, McKenney CM, Ruoslahti E, Cleland AN. A high-throughput label-free nanoparticle analyser. *Nat Nanotechnol* 2011; **6**: 308–13.
29 van der Pol E, ISTH-SSC-VB Working Group, Hau C, Sturk A, van Leeuwen TG, Nieuwland R, Coumans FAW. Standardization of extracellular vesicle measurements by flow cytometry through vesicle diameter approximation. *J Thromb Haemost* 2018; **16**: 1236–45.
30 de Rond L, van der Pol E, Hau CM, Varga Z, Sturk A, van Leeuwen TG, Nieuwland R, Coumans FAW. Comparison of generic fluorescent markers for detection of extracellular vesicles by flow cytometry. *Clin Chem* 2018; **64**: 680–89.
31 Pálmai M, Nagy LN, Mihály J, Varga Z, Tárkányi G, Mizsei R, Szigyártó IC, Kiss T, Kremmer T, Bóta A. Preparation, purification, and characterization of aminopropyl-functionalized silica sol. *J Colloid Interface Sci* 2013; **390**: 34–40.
32 Mitra K, Ubarretxena-Belandia I, Taguchi T, Warren G, Engelman DM. Modulation of the bilayer thickness of exocytic pathway membranes by membrane proteins rather than cholesterol. *Proc Natl Acad Sci USA* 2004; **101**: 4083–8.
33 Lewis BA, Engelman DM. Lipid bilayer thickness varies linearly with acyl chain length in fluid phosphatidylcholine vesicles. *J Mol Biol* 1983; **166**: 211–17.
34 Balgavý P, Dubnicková M, Kucerka N, Kiselev MA, Yaradaikin SP, Uhríková D. Bilayer thickness and lipid interface area in unilamellar extruded 1,2-diacylphosphatidylcholine liposomes: a small-angle neutron scattering study. *Biochim Biophys Acta* 2001; **1512**: 40–52.
35 Tahara Y, Fujiyoshi Y. A new method to measure bilayer thickness: cryo-electron microscopy of frozen hydrated liposomes and image simulation. *Micron* 1994; **25**: 141–9.
36 Lambert O, Gerke V, Bader MF, Porte F, Brisson A. Structural analysis of junctions formed between lipid membranes and several annexins by cryo-electron microscopy. *J Mol Biol* 1997; **272**: 42–55.
37 Horváth R, Fricsovszky G, Papp E. Application of the optical waveguide lightmode spectroscopy to monitor lipid bilayer phase transition. *Biosens Bioelectron* 2003; **18**: 415–28.
38 Ducharme D, Max JJ, Salesse C, Leblanc RM. Ellipsometric study of the physical states of phosphatidylcholines at the air–water interface. *J Phys Chem* 1990; **94**: 1925–32.
39 Mashaghi A, Swann M, Popplewell J, Textor M, Reimhult E. Optical anisotropy of supported lipid structures probed by waveguide spectroscopy and its application to study of supported lipid bilayer formation kinetics. *Anal Chem* 2008; **80**: 3666–76.
40 Kienle DF, de Souza JV, Watkins EB, Kuhl TL. Thickness and refractive index of DPPC and DPPE monolayers by multiple-beam interferometry. *Anal Bioanal Chem* 2014; **406**: 4725–33.
41 Barer R, Joseph S. Refractometry of living cells: part I. Basic principles. *J Cell Sci* 1954; **3**: 399–423.
42 van der Pol E, de Rond L, Coumans FAW, Gool EL, Böing AN, Sturk A, Nieuwland R, van Leeuwen TG. Absolute sizing and label-free identification of extracellular vesicles by flow cytometry. *Nanomedicine* 2018; **14**: 801–10.
43 Shang J, Gao X. Nanoparticle counting: towards accurate determination of the molar concentration. *Chem Soc Rev* 2014; **43**: 7267–78.
44 *Handbook of Optics* Vol. 4, 3rd edn. New York: McGraw-Hill, 2009.
45 Daimon M, Masumura A. Measurement of the refractive index of distilled water from the near-infrared region to the ultraviolet region. *Appl Opt* 2007; **46**: 3811–20.
46 Valkonen S, van der Pol E, Böing A, Yuana Y, Yliperttula M, Nieuwland R, Laitinen S, Siljander PRM. Biological reference materials for extracellular vesicle studies. *Eur J Pharm Sci* 2017; **98**: 4–16.